JPE 8-1-9

Frequency Characteristics of the Synchronous-Frame Based *D-Q* Methods for Active Power Filters

WANG Xiaoyu†, LIU Jinjun*, HU Jinku*, MENG Yuji* and YUAN Chang*

†*School of Electrical Engineering, Xi'an Jiaotong University, Xi'an, China

ABSTRACT

The *d-q* harmonic detecting algorithms are dominant methods to generate current references for active power filters (APF). They are often implemented in the synchronous frame and time domain. This paper researches the frequency characteristics of *d-q* synchronous transformations, which are closely related to the analysis and design issues of control system. Intuitively, the synchronous transformation is explained with amplitude modulation (AM) in this paper. Then, the synchronous filter is proven to be a time-invariant and linear system, and its transfer function matrix is derived in the stationary frames. These frequency-domain models imply that the synchronous transformation has an equivalent effect of frequency transformation. It is because of this feature, the *d-q* method achieves band-pass characteristics with the low pass filters in the synchronous frame at run time. To simplify these analytical models, an instantaneous positive-negative sequence frame is proposed as expansion of traditional symmetrical components theory. Furthermore, the synchronous filter is compared with the traditional bind-pass filters based on these frequency-domain analytical models. The *d-q* harmonic detection methods are also improved to eliminate the inherent coupling effect of synchronous transformation. Typical examples are given to verify previous analysis and comparison. Simulation and experimental results are also provided for verification.

Keywords: instantaneous reactive power theory, *d-q* method, harmonics detection, active power filter, synchronous filter

1. Introduction

Active power filters (APF) have been one of the most competitive solutions to suppress power system harmonics and improve power quality[1][2]. For the control of APF, current reference generation scheme plays a crucial role [2]. The key to these schemes is harmonics detection, and existing approaches can be divided into time-domain methods and frequency-domain methods[3]. The time-domain methods are the dominant algorithms after the proposal of instantaneous power theory[4][5], such as "*p-q* method" based on *p-q* theory [5], "*d-q* method" in *d-q* synchronous frame[6][7], and flux-based control method etc[8]. Although these time-domain methods are popular and easy to implement especially in digital controllers, there are still several design-related theoretical questions that has not been clearly answered:

• Since the essential aim of *d-q* synchronous-frame current reference generation methods for APF is

Manuscript received Nov. 12, 2007; revised Dec. 11, 2007
† Corresponding Author: xywang@ieee.org
Tel: +86-29-82667858, Fax: +86-29-82665223, Xi'an Jiaotong Univ.
*School of Electrical Engineering, Xi'an Jiaotong University, 28 West Xianning Road, Xi'an, Shaanxi 710049 China

separating the fundamental current and the harmonic current, what are their filtering characteristics in frequency domain?

- What are the differences and relationship between *d-q* synchronous-frame methods and the traditional filter designed in frequency domain?
- What design allows the low pass filter (LPF) in synchronous frame to satisfy the harmonics detection requirements in the stationary frame?
- The loop gain is very important for design and analysis of the close-loop performance. This raises the question of how we can evaluate the close-loop gains of the control systems based on *d-q* synchronous frame?

All these questions are related to the frequency characteristics of synchronous transformation. In 1993, a frequency analytical model of the *p-q* method was derived and employed in the stability analysis of series active power filters (SAPF)[9]. However it is too complicated and too academic for electrical engineers in practical application. In the research of current close-loop regulators, the synchronous proportional integral (PI) regulator was analyzed in frequency domain, and a stationary PI (or resonant-PI) regulator was subsequently proposed[10][11]. But this discussion focused mainly on current regulators with a lack of physical meaning and explanation.

In this paper, the synchronous transformation is intuitively explained with amplitude modulation (AM) in communication theory. A pair of synchronous transformations is proven to be time-invariant and linear although each one is nonlinear and time-variant. So the synchronous filter can be modeled with transfer functions in frequency domain and stationary frame. The frequency-domain analytical models imply that the synchronous transformation has an equivalent effect of frequency transformation, by which several band-pass filters (BPF) are achieved with the spectral transformation of two low pass filters at run time.

With the stationary frequency analytical models, the frequency characteristics of *d-q* methods are investigated in detail. To simplify the analytical model, an instantaneous positive-negative sequence frame is proposed as an expansion of symmetrical components theory. A simpler frequency analytical model is then obtained in instantaneous positive-negative sequence frame. With intuitive physical meanings, the model in instantaneous positive-negative sequence frame is easy to understand and apply.

Based on these analytical models, the *d-q* synchronous-frame current reference generation methods are compared with the traditional band-pass filters. Furthermore, stationary filters were proposed to eliminate the inherent coupling effect of synchronous transformation.

Typical examples are given to verify previous analysis and comparison. Simulation and experimental results are also given.

2. Review and Novel Intuitive Explanation of Synchronous-Frame *D-Q* Methods

Fig. 1 shows the widely used synchronous-frame *d-q* current reference generation methods for Active Power Filter, where i_L is the load current, i_C^* is the current reference to APF, and the transformation operators are

$$C_{32}=\sqrt{\frac{2}{3}}\begin{bmatrix}1 & -\frac{1}{2} & -\frac{1}{2}\\ 0 & \frac{\sqrt{3}}{2} & -\frac{\sqrt{3}}{2}\end{bmatrix},\quad C=\begin{bmatrix}\cos\omega_0 t & \sin\omega_0 t\\ -\sin\omega_0 t & \cos\omega_0 t\end{bmatrix},$$

$$C^{-1}=\begin{bmatrix}\cos\omega_0 t & -\sin\omega_0 t\\ \sin\omega_0 t & \cos\omega_0 t\end{bmatrix},\quad C_{32}=C_{32}^T. \tag{1}$$

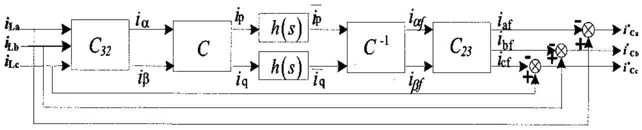

Fig. 1 Synchronous-Frame Based *d-q* Methods for APF

In these synchronous-frame *d–q* methods, voltage and current signals are transformed to a synchronously rotating frame, in which fundamental quantities become DC quantities, and then the harmonic compensating commands are easily extracted. The key operation of synchronous transformation is the multiple of the signals with trigonometric function, which is much like the process of amplitude modulation. Before amplitude modulation theory is employed to explain the synchronous frame current generation scheme, basic principle of amplitude modulation is reviewed.

Let $F(\omega)$ represents the spectrum of the original signal $f(t)$, then the spectrum of the amplitude-modulated signal becomes

$$\begin{aligned} S(\omega) &= \mathcal{F}\left(s(t)\right) = \mathcal{F}\left(f(t)\cdot\cos\omega_0 t\right) \\ &= \mathcal{F}\left(f(t)\frac{e^{j\omega_0 t}+e^{-j\omega_0 t}}{2}\right) \\ &= \frac{1}{2}\left(F(\omega-\omega_0)+F(\omega+\omega_0)\right) \end{aligned} \tag{2}$$

Fig.2 compares the original signal and its corresponding modulated signal with amplitude in both time domain and frequency domain. With amplitude modulation, the spectrum of the original signal $F(\omega)$ is transformed to 50Hz higher (given that line frequency is 50Hz) as shown in Fig. 2.

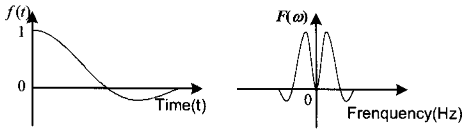

(a) Original signal

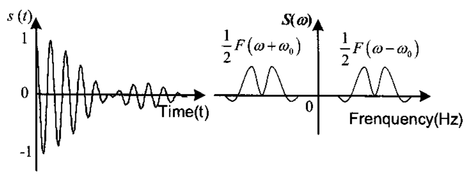

(b) Modulated signal with amplitude modulation (AM)

Fig. 2 Illustration of amplitude modulation (AM) with waveforms and spectrum plots

Similar to the amplitude modulation, the *d-q* harmonics detection algorithm achieved stationary band-pass filters with two low pass filters in synchronous frame. Fig. 3 intuitively illustrates the synchronous-frame *d-q* current generation scheme with amplitude modulation. The first synchronous transformation lowers the current spectrum to 50Hz, which is much like amplitude demodulation. After the process of lower pass filtering in the synchronous frame, the current spectrum increases to 50Hz higher, and this is much like amplitude modulation. In this way, the low pass filter in the synchronous frame actually filters out the signal at the fundamental frequency (50Hz), so the equivalent effect of the synchronous-frame low pass filter is the band-pass filter in stationary frame. Detail analysis and precise derivation will be given in the next section.

3. Frequency-Domain Analytical Models in Stationary Frames

The synchronous filter is the key part of the synchronous-frame based *d-q* methods for APF. In the view of the system, the synchronous filter could be modeled as a black box, shown as Fig. 4. With the intuitive explanation with amplitude modulation, the synchronous transformation is analyzed in frequency domain in this section and a frequency analytical model of synchronous filter is given.

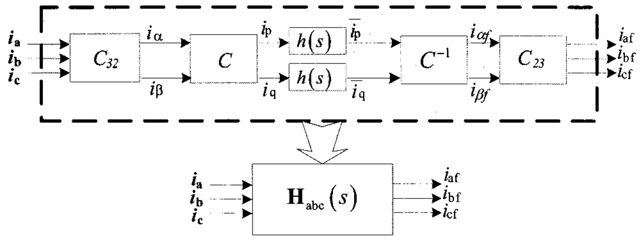

Fig. 4 Modeling of synchronous filter as a black box in frequency domain

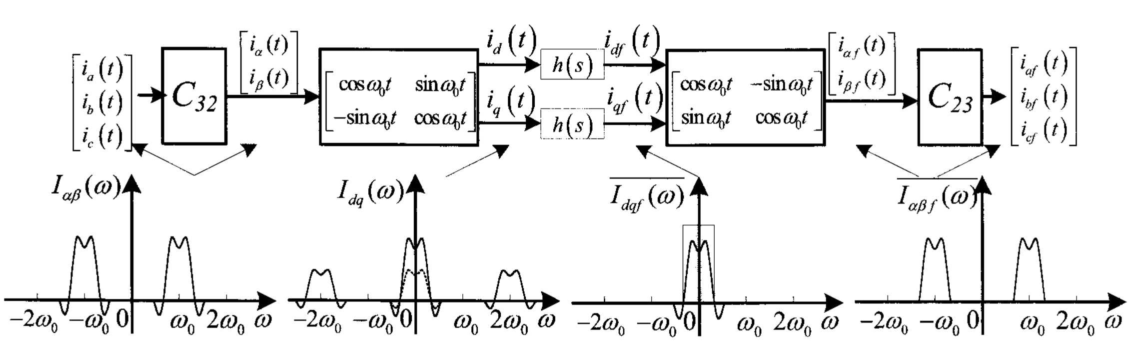

Fig. 3 Novel and intuitive explanation of *d-q* synchronous frame current generation scheme with amplitude modulation (AM)

Because $\alpha\beta$ transformation is a linear transformation, the key of the discussion is the modeling of a pair of synchronous transformations. Consider the transfer function matrix of $\mathbf{H}_{\alpha\beta}(s)$ in $\alpha\beta$ stationary frame

$$\begin{bmatrix} i_{\alpha f}(s) \\ i_{\beta f}(s) \end{bmatrix} = \mathbf{H}_{\alpha\beta}(s)\begin{bmatrix} i_{\alpha}(s) \\ i_{\beta}(s) \end{bmatrix} = \begin{bmatrix} \frac{i_{\alpha f}(s)}{i_{\alpha}(s)} & \frac{i_{\alpha f}(s)}{i_{\beta}(s)} \\ \frac{i_{\beta f}(s)}{i_{\alpha}(s)} & \frac{i_{\beta f}(s)}{i_{\beta}(s)} \end{bmatrix}\begin{bmatrix} i_{\alpha}(s) \\ i_{\beta}(s) \end{bmatrix} \quad (3)$$

where $\mathbf{I}_{\alpha\beta}(s) = \left[i_{\alpha}(s) \quad i_{\beta}(s)\right]^{\mathrm{T}}$ is the input vector of currents in $\alpha\beta$ frame, and $\mathbf{I}_{\alpha\beta f}(s) = \left[i_{\alpha f}(s) \quad i_{\beta f}(s)\right]^{\mathrm{T}}$ is the corresponding fundamental component of currents. All elements are in terms of Laplace transformation.

In the appendix of this paper, the synchronous filter is proven to be a time-invariant linear transformation, and the transfer function matrix of $\mathbf{H}_{\alpha\beta}(s)$ is derived as

$$\mathbf{H}_{\alpha\beta}(s) = \begin{bmatrix} \frac{1}{2}\left[h(s+j\omega_0)+h(s-j\omega_0)\right] & -j\frac{1}{2}\left[h(s+j\omega_0)-h(s-j\omega_0)\right] \\ j\frac{1}{2}\left[h(s+j\omega_0)-h(s-j\omega_0)\right] & \frac{1}{2}\left(h(s+j\omega_0)+h(s-j\omega_0)\right) \end{bmatrix} = \begin{bmatrix} a & -jb \\ jb & a \end{bmatrix} \quad (4)$$

with a and b given by

$$a = \frac{1}{2}\left(h(s+j\omega_0)+h(s-j\omega_0)\right) \quad (5)$$

$$b = \frac{1}{2}\left(h(s+j\omega_0)-h(s-j\omega_0)\right) \quad (6)$$

where $h(s)$ is low pass filter in d-q synchronous frame. This means the LPF of $h(s)$ is transformed to a band-pass filter with frequency conversion to 50Hz higher.

Fig. 5 illustrates this analytical model of $\mathbf{H}_{\alpha\beta}(s)$ in stationary frame and frequency domain. From Fig. 5, unexpected coupling effect is found in synchronous-frame d-q methods, which makes the design of close-loop regulator complicated. Some modifications have been proposed to decouple the d-q methods [12].

It is more direct to investigate the transfer function matrix of d-q methods in a-b-c stationary frame as

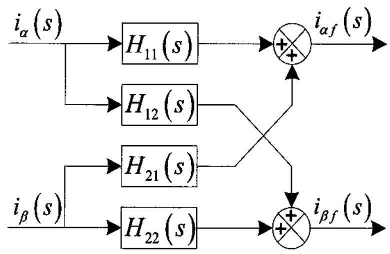

Fig. 5 Modeling of synchronous filter in frequency domain and stationary frame

$$\begin{bmatrix} i_{af}(s) \\ i_{bf}(s) \\ i_{cf}(s) \end{bmatrix} = \mathbf{H}_{\mathrm{abc}}(s)\begin{bmatrix} i_{a}(s) \\ i_{b}(s) \\ i_{c}(s) \end{bmatrix} \quad (7)$$

where $i_a(s)$, $i_b(s)$ and $i_c(s)$ are three phase currents, and $i_{af}(s)$, $i_{bf}(s)$ and $i_{cf}(s)$ are the corresponding fundamental components of currents. All elements are in terms of Laplace transformation.

In the a-b-c stationary frame, the frequency-domain analytical model $\mathbf{H}_{\mathrm{abc}}(s)$ can be obtained from $\mathbf{H}_{\alpha\beta}(s)$

$$\begin{aligned} \mathbf{H}_{\mathrm{abc}}(s) &= C_{23}\mathbf{H}_{\alpha\beta}(s)C_{32} \\ &= C_{23}\begin{bmatrix} a & -jb \\ jb & a \end{bmatrix}C_{32} \\ &= \begin{bmatrix} \frac{2}{3}a & -\frac{1}{3}a-j\frac{\sqrt{3}}{3}b & -\frac{1}{3}a+j\frac{\sqrt{3}}{3}b \\ -\frac{1}{3}a+j\frac{\sqrt{3}}{3}b & \frac{2}{3}a & -\frac{1}{3}a-j\frac{\sqrt{3}}{3}b \\ -\frac{1}{3}a-j\frac{\sqrt{3}}{3}b & -\frac{1}{3}a+j\frac{\sqrt{3}}{3}b & \frac{2}{3}a \end{bmatrix} \end{aligned} \quad (8)$$

with a and b given by (5) and (6).

It is clear in (8) that the synchronous filter has coupling effect among three phases, which means the synchronous filter is only suitable for symmetrical systems.

4. Frequency-Domain Analytical Model in Positive-Negative Sequence Frame

To simplify previous frequency-domain analytical models of d-q methods, an instantaneous positive-negative sequence frame is proposed as an expansion of symmetrical components theory.

Define

$$\begin{bmatrix} i^{+}(s) \\ i^{-}(s) \\ i^{0}(s) \end{bmatrix} = \frac{1}{\sqrt{3}} \begin{bmatrix} 1 & -\frac{1}{2}+\frac{\sqrt{3}}{2}j & -\frac{1}{2}-\frac{\sqrt{3}}{2}j \\ 1 & -\frac{1}{2}-\frac{\sqrt{3}}{2}j & -\frac{1}{2}+\frac{\sqrt{3}}{2}j \\ 1 & 1 & 1 \end{bmatrix} \begin{bmatrix} i_a(s) \\ i_b(s) \\ i_c(s) \end{bmatrix} \tag{9}$$

$$\begin{bmatrix} i_a(s) \\ i_b(s) \\ i_c(s) \end{bmatrix} = \frac{1}{\sqrt{3}} \begin{bmatrix} 1 & 1 & 1 \\ -\frac{1}{2}-\frac{\sqrt{3}}{2}j & -\frac{1}{2}+\frac{\sqrt{3}}{2}j & 1 \\ -\frac{1}{2}+\frac{\sqrt{3}}{2}j & -\frac{1}{2}-\frac{\sqrt{3}}{2}j & 1 \end{bmatrix} \begin{bmatrix} i^{+}(s) \\ i^{-}(s) \\ i^{0}(s) \end{bmatrix} \tag{10}$$

where $\boldsymbol{i}_a(s)$, $\boldsymbol{i}_b(s)$ and $\boldsymbol{i}_c(s)$ are three-phase currents in terms of Laplace transformation, and $i^{+}(s)$, $i^{-}(s)$ and $i^{0}(s)$ are the positive, negative and zero sequence separately.

In this positive-negative sequence frame, the frequency analytical model becomes very simple without coupling as

$$\begin{cases} i_f^{+}(s) = h(s - j\omega_0) \times i^{+}(s) \\ i_f^{-}(s) = h(s + j\omega_0) \times i^{-}(s) \end{cases} \tag{11}$$

where i_f^{+} and i_f^{-} indicate the positive and negative sequences of fundamental currents respectively.

5. Analytical Example

This section gives an example for demonstration. Assume that the low pass filter in d-q methods is second order with the transfer function given by

$$h(s) = \frac{1}{\left(\dfrac{s}{\omega_C}\right)^2 + 2\varsigma \dfrac{s}{\omega_C} + 1} \tag{12}$$

where $\omega_C = 2\pi \cdot 50$ rad/s, $\varsigma = \dfrac{1}{\sqrt{2}}$.

Fig. 6 shows its Bode plot and Nyquist plot. Here the axis is given in linear scale.

With previous analytical model of (4), the $\alpha\beta$ -frame transfer function matrix of d-q methods can be obtained by transformation of (12) as

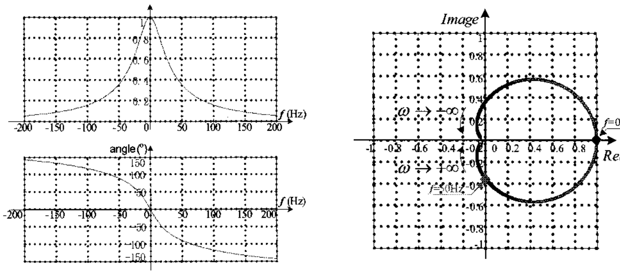

(a) Bode plot (b) Nyquist plot

Fig. 6 Spectrum of a second-order low pass filter

$$\mathbf{H}_{\alpha\beta}(s) = \begin{bmatrix} \frac{1}{2}\left[h(s+j\omega_0)+h(s-j\omega_0)\right] & -j\frac{1}{2}\left[h(s+j\omega_0)-h(s-j\omega_0)\right] \\ j\frac{1}{2}\left[h(s+j\omega_0)-h(s-j\omega_0)\right] & \frac{1}{2}\left(h(s+j\omega_0)+h(s-j\omega_0)\right) \end{bmatrix}$$
$$= \frac{\omega_C^2}{\Delta} \begin{bmatrix} s^2 + 2\zeta\omega_C \cdot s + \omega_C^2 - \omega_0^2 & -2\omega_0(s+\omega_C) \\ 2\omega_0(s+\omega_C) & s^2 + 2\zeta\omega_C \cdot s + \omega_C^2 - \omega_0^2 \end{bmatrix} \tag{13}$$

where

$$\Delta = s^4 + 4\zeta\omega_C \cdot s^3 + \left(4\zeta^2\omega_C^2 + 2\omega_0^2 + 2\omega_C^2\right) \cdot s^2$$
$$+4\left(\omega_0^2\zeta\omega_C + \zeta\omega_C^3\right) \cdot s + 4\zeta^2\omega_C^2\omega_0^2 + \left(\omega_0^2 - \omega_C^2\right)^2$$

Fig. 7 and Fig. 8 show the Bode plot and Nyquist plot of the diagonal element and coupling element respectively of (13). These plots can be directly obtained from Fig. 6 by frequency transformation.

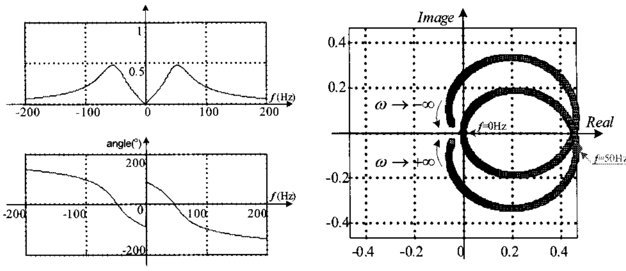

(a) Bode plot (b) Nyquist plot

Fig. 7 Equivalent spectrum of the diagonal element in $\mathbf{H}_{\alpha\beta}(s)$

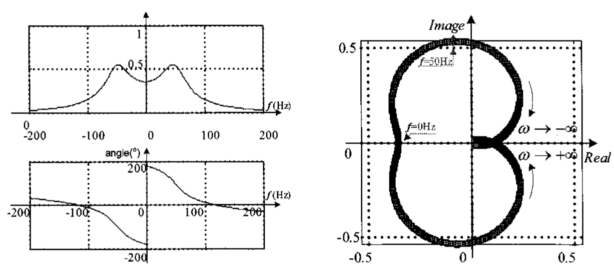

(a) Bode plot (b) Nyquist plot

Fig. 8 Equivalent spectrum of the coupling element in $\mathbf{H}_{\alpha\beta}(s)$

6. Comparisons of Reference Generation Methods in Frequency Domain

Based on the previous frequency-domain analytical models, the time-domain *d-q* synchronous filter can be compared with the traditional band-pass filter, which are generally designed in frequency-domain.

6.1 Comparison with traditional band-pass filter

The tradition frequency-domain band-pass filters have many types and may be implemented with either analog or digital devices. The most popular and practical design method is spectral transformation from a uniformed low pass filter, with the mapping function given by

$$s \rightarrow Q\left(\frac{s}{\omega_0}+\frac{\omega_0}{s}\right) \tag{14}$$

where ω_0 is the target center frequency of BPF, and Q is the quality factor of the target band-pass filter.

In comparison of this traditional design method for band-pass filters, the *d-q* frame synchronous filter also achieves band-pass characteristics with lower pass filters. Their difference is that the traditional band-pass filter is transformed from LPF in the design stage, while the synchronous filter performs in the run-time.

Fig. 9 comparatively shows the Bode plots of the synchronous filter and traditional band-pass filter. Given the same prototype low pass filter, the *d-q* frame synchronous filter and the traditional band-pass filter have the similar frequency-domain characteristics. In this case, their differences appear only below –20dB.

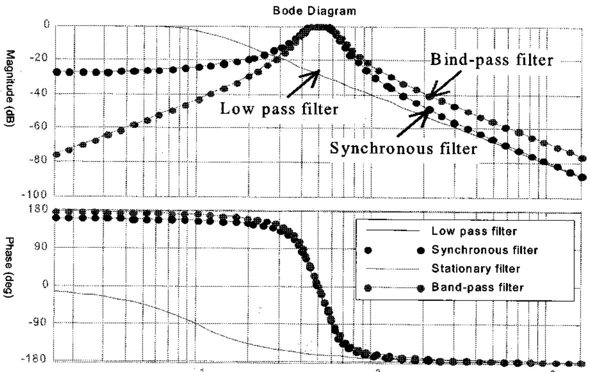

Fig. 9 Bode plots comparison of different band-pass filters

With deeper analysis of Fig. 9, it can be found that the spectrum of the traditional BPF is geometrically symmetrical with the frequency axis in the log scale because the bind-pass filter transforms the low pass filter with the mapping function given by (14), while the spectrum of *d-q* synchronous scheme is mathematically symmetrical with the frequency axis in the linear scale.

6.2 New decoupled stationary *d-q* method

As shown in Fig. 5, the *d-q* methods have inherent coupling effect from the synchronous transformation. The *d-q* methods would be decoupled if the references were calculated in stationary frame with their frequency analytical models. The decoupled stationary-frame *d-q* method in the stationary frame can be easily obtained with the diagonal of $\mathbf{H}_{abc}(s)$ or $\mathbf{H}_{\alpha\beta}(s)$. This modification expands the *d-q* methods from symmetrical systems to unsymmetrical systems.

It is generally easier to design and implement the *d-q* method in a synchronous frame than stationary frame. But with the rapid advancement of powerful yet cheap digital signal processors (DSP), some popular interpretations of synchronous filters should be updated.

6.3 Simulation results

Comparative simulations were held to detect the fundamental component from the currents of a three-phase rectifier. All band-pass filters take the second-order LPF of (12) as target filter.

Fig. 10 shows the simulation results. Each filter obtains similar results in both steady state and transient state.

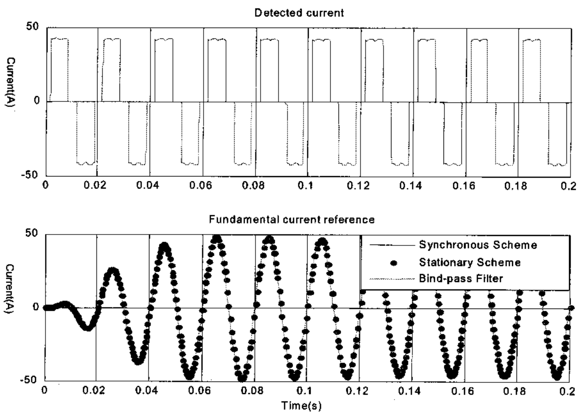

Fig. 10 Comparison with time-domain simulation

7. Experimental results

To verify the previous analysis, the synchronous filter, the traditional bind-pass filter and the proposed stationary filter are realized in DSP (TMS320F2812) and their performances are compared within the experiments. Fig. 11 shows the experimental configuration.

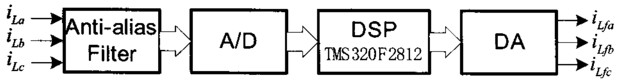

Fig. 11 Experimental configuration based on DSP

The inputs are currents of a three-phase rectifier with inductor, which is the typical harmonic source of power quality problems. Fig. 12 shows the experimental result in the symmetrical system. All the filters show similar performance in both transient and steady states.

Fig. 13 shows the result when the input currents are unsymmetrical. In this case, the synchronous filter can only generate symmetrical output because of the unexpected coupling effect, while the traditional bind-pass filter and the proposed stationary filter work well in the unsymmetrical system.

8. Conclusion

The synchronous transformation was intuitively explained with amplitude modulation and frequency transformation. The transfer function matrix of the synchronous filter was derived in the frequency domain and stationary frames. An instantaneous positive-negative sequence frame was proposed as an expansion of symmetrical components theory, in which the frequency-domain model of *d-q* methods is significantly simplified. These frequency-domain analytical models imply that the synchronous-frame *d-q* methods obtain the current harmonics with spectrum transformation of low pass filter at run time.

Based on these frequency analytical models, the synchronous filter was compared with the traditional bind-pass filters. Furthermore, stationary filters were proposed to eliminate the inherent coupling effect of

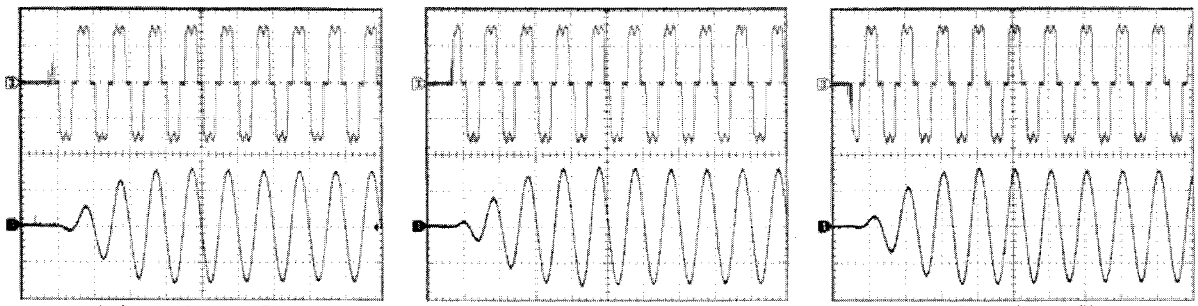

a) *d-q* synchronous filter b) Traditional bind-pass filter c) 4-order stationary filter

Up curve: load current of phase a (2A/div); Down curve: detected fundamental current of phase a (2A/div). Horizon axis: time: (20ms/div).

Fig. 12 Experimental results in symmetrical system

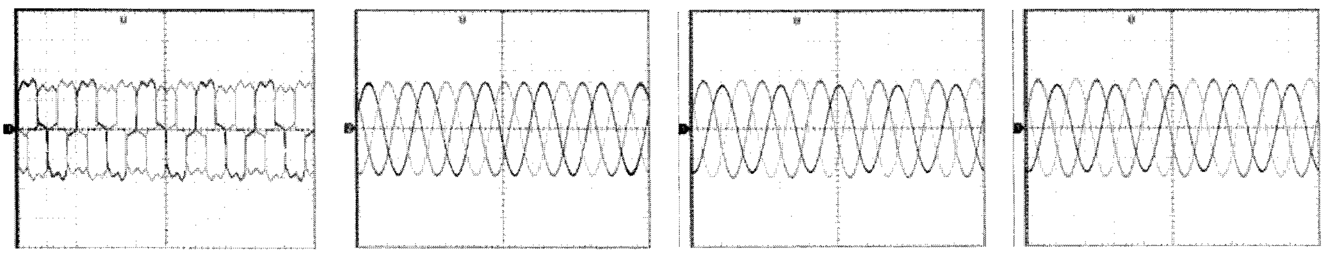

a) Unsymmetrical load current b) Output of synchronous filter c) Output of traditional BPF d) Output of stationary filter

Horizon axis: time (10ms/div). Vertical axis: currents (2A/div).

Fig. 13 Experimental results of three-phase current in unsymmetrical system synchronous transformation. Typical examples are given to verify previous analysis and comparison. Simulation and experimental results are also provided for verification.

Appendix

The transfer function $\mathbf{H}_{\alpha\beta}(s)$ in $\alpha\beta$ stationary frame is derived in detail in the appendix.

Define the stationary frame transfer function $\mathbf{H}_{\alpha\beta}(s)$ as

$$\begin{bmatrix} i_{\alpha f}(s) \\ i_{\beta f}(s) \end{bmatrix} = \mathbf{H}_{\alpha\beta}(s)\begin{bmatrix} i_{\alpha}(s) \\ i_{\beta}(s) \end{bmatrix} = \begin{bmatrix} \frac{i_{\alpha f}(s)}{i_{\alpha}(s)} & \frac{i_{\alpha f}(s)}{i_{\beta}(s)} \\ \frac{i_{\beta f}(s)}{i_{\alpha}(s)} & \frac{i_{\beta f}(s)}{i_{\beta}(s)} \end{bmatrix}\begin{bmatrix} i_{\alpha}(s) \\ i_{\beta}(s) \end{bmatrix}$$

where the input vector is $\mathbf{I}_{\alpha\beta}(s)=\begin{bmatrix} i_{\alpha}(s) & i_{\beta}(s)\end{bmatrix}^{\mathrm{T}}$ and the output vector $\mathbf{I}_{\alpha\beta f}(s)=\begin{bmatrix} i_{\alpha f}(s) & i_{\beta f}(s)\end{bmatrix}^{\mathrm{T}}$ is the fundamental component of input vector.

First, the time domain $\mathbf{I}_{dq}(t)=\begin{bmatrix} i_{d}(t) & i_{q}(t)\end{bmatrix}^{\mathrm{T}}$ is transformed to (15).

$$\begin{aligned}\begin{bmatrix} i_d(t) \\ i_q(t) \end{bmatrix} &= \begin{bmatrix} \cos\omega_0 t & \sin\omega_0 t \\ -\sin\omega_0 t & \cos\omega_0 t \end{bmatrix}\begin{bmatrix} i_\alpha(t) \\ i_\beta(t) \end{bmatrix} \\ &= \begin{bmatrix} \frac{e^{j\omega_0 t}+e^{-j\omega_0 t}}{2} & \frac{j}{2}\left(e^{-j\omega_0 t}-e^{j\omega_0 t}\right) \\ -\frac{j}{2}\left(e^{-j\omega_0 t}-e^{j\omega_0 t}\right) & \frac{e^{j\omega_0 t}+e^{-j\omega_0 t}}{2} \end{bmatrix}\begin{bmatrix} i_\alpha(t) \\ i_\beta(t) \end{bmatrix} \\ &= \frac{1}{2}e^{j\omega_0 t}\begin{bmatrix} 1 & -j \\ j & 1 \end{bmatrix}\begin{bmatrix} i_\alpha(t) \\ i_\beta(t) \end{bmatrix} + \frac{1}{2}e^{-j\omega_0 t}\begin{bmatrix} 1 & j \\ -j & 1 \end{bmatrix}\begin{bmatrix} i_\alpha(t) \\ i_\beta(t) \end{bmatrix}\end{aligned} \tag{15}$$

Applying Laplace transformation, (15) becomes

$$\begin{bmatrix} i_d(s) \\ i_q(s) \end{bmatrix} = \frac{1}{2}\begin{bmatrix} 1 & -j \\ j & 1 \end{bmatrix}\begin{bmatrix} i_\alpha(s-j\omega_0) \\ i_\beta(s-j\omega_0) \end{bmatrix} + \frac{1}{2}\begin{bmatrix} 1 & j \\ -j & 1 \end{bmatrix}\begin{bmatrix} i_\alpha(s+j\omega_0) \\ i_\beta(s+j\omega_0) \end{bmatrix} \tag{16}$$

After the low pass filter in synchronous frame,

$$\begin{aligned}\begin{bmatrix} i_{df}(s) \\ i_{qf}(s) \end{bmatrix} &= \begin{bmatrix} h(s) & 0 \\ 0 & g(s) \end{bmatrix}\begin{bmatrix} i_d(s) \\ i_q(s) \end{bmatrix} \\ &= \frac{1}{2}\begin{bmatrix} 1 & -j \\ j & 1 \end{bmatrix}\begin{bmatrix} h(s)\cdot i_\alpha(s-j\omega_0) \\ g(s)\cdot i_\beta(s-j\omega_0) \end{bmatrix} + \frac{1}{2}\begin{bmatrix} 1 & j \\ -j & 1 \end{bmatrix}\begin{bmatrix} h(s)\cdot i_\alpha(s+j\omega_0) \\ g(s)\cdot i_\beta(s+j\omega_0) \end{bmatrix}\end{aligned} \tag{17}$$

Similar to the first synchronous transformation as (15) and (16), the fundamental component as output vector $\mathbf{I}_{\alpha\beta f}(s)$ is obtained in terms of Laplace transformation

$$\begin{bmatrix} i_{\alpha f}(s) \\ i_{\beta f}(s) \end{bmatrix} = \frac{1}{2}\begin{bmatrix} 1 & -j \\ j & 1 \end{bmatrix}\begin{bmatrix} i_{df}(s+j\omega_0) \\ i_{qf}(s+j\omega_0) \end{bmatrix} + \frac{1}{2}\begin{bmatrix} 1 & j \\ -j & 1 \end{bmatrix}\begin{bmatrix} i_{df}(s-j\omega_0) \\ i_{qf}(s-j\omega_0) \end{bmatrix} \tag{18}$$

Substitution of (16) and (17) to (18) yields (19).

$$\begin{bmatrix} i_{\alpha f}(s) \\ i_{\beta f}(s) \end{bmatrix} = \frac{1}{2}\begin{bmatrix} 1 & -j \\ j & 1 \end{bmatrix}\begin{bmatrix} i_{df}(s+j\omega_0) \\ i_{qf}(s+j\omega_0) \end{bmatrix} + \frac{1}{2}\begin{bmatrix} 1 & j \\ -j & 1 \end{bmatrix}\begin{bmatrix} i_{df}(s-j\omega_0) \\ i_{qf}(s-j\omega_0) \end{bmatrix} \tag{19}$$

Because of the equation

$$\begin{bmatrix} 1 & -j \\ j & 1 \end{bmatrix}\begin{bmatrix} 1 & j \\ -j & 1 \end{bmatrix} \equiv \mathbf{0} \tag{20}$$

(19) is simplified to (21). Various forms of the transfer function can be obtained as (22) in $\alpha\beta$ stationary frame. Each of the expressions can be explained with specific physical meanings, but here in this paper the expression of (4) is selected for reasons of simplicity.

$$\begin{cases} \mathbf{H}_{\alpha\beta}(s) = \frac{1}{2}\begin{bmatrix} 1 & -j \\ j & 1 \end{bmatrix}\begin{bmatrix} h(s+j\omega_0) \\ g(s+j\omega_0) \end{bmatrix} + \frac{1}{2}\begin{bmatrix} 1 & j \\ -j & 1 \end{bmatrix}\begin{bmatrix} h(s+j\omega_0) \\ g(s-j\omega_0) \end{bmatrix} \\ \mathbf{H}_{\alpha\beta}(s) = \begin{bmatrix} \frac{1}{2}\left[h(s+j\omega_0)+h(s-j\omega_0)\right] & -j\frac{1}{2}\left[g(s+j\omega_0)-g(s-j\omega_0)\right] \\ j\frac{1}{2}\left[h(s+j\omega_0)-h(s-j\omega_0)\right] & \frac{1}{2}\left(g(s+j\omega_0)+g(s-j\omega_0)\right) \end{bmatrix} \\ \mathbf{H}_{\alpha\beta}(s) = \mathrm{L}\left\{\begin{bmatrix} \cos\omega_0 t & -\sin\omega_0 t \\ \sin\omega_0 t & \cos\omega_0 t \end{bmatrix}\begin{bmatrix} h(t) \\ g(t) \end{bmatrix}\right\} \end{cases} \tag{22}$$

$$\begin{aligned}\begin{bmatrix} i_{\alpha f}(s) \\ i_{\beta f}(s) \end{bmatrix} &= \frac{1}{4}\begin{bmatrix} 1 & -j \\ j & 1 \end{bmatrix}\begin{bmatrix} 1 & -j \\ j & 1 \end{bmatrix}\begin{bmatrix} h(s+j\omega_0)\cdot i_\alpha(s) \\ g(s+j\omega_0)\cdot i_\beta(s) \end{bmatrix} + \underbrace{\frac{1}{4}\begin{bmatrix} 1 & -j \\ j & 1 \end{bmatrix}\begin{bmatrix} 1 & j \\ -j & 1 \end{bmatrix}\begin{bmatrix} h(s+j\omega_0)\cdot i_\alpha(s+j2\omega_0) \\ g(s+j\omega_0)\cdot i_\beta(s+j2\omega_0) \end{bmatrix}}_{=0} \\ &+ \underbrace{\frac{1}{4}\begin{bmatrix} 1 & j \\ -j & 1 \end{bmatrix}\begin{bmatrix} 1 & -j \\ j & 1 \end{bmatrix}\begin{bmatrix} h(s-j\omega_0)\cdot i_\alpha(s-j2\omega_0) \\ g(s-j\omega_0)\cdot i_\beta(s-j2\omega_0) \end{bmatrix}}_{=0} + \frac{1}{4}\begin{bmatrix} 1 & j \\ -j & 1 \end{bmatrix}\begin{bmatrix} 1 & j \\ -j & 1 \end{bmatrix}\begin{bmatrix} h(s-j\omega_0)\cdot i_\alpha(s) \\ g(s-j\omega_0)\cdot i_\beta(s) \end{bmatrix} \\ &= \begin{bmatrix} \frac{1}{2}\left[h(s+j\omega_0)+h(s-j\omega_0)\right] & -j\frac{1}{2}\left[g(s+j\omega_0)-g(s-j\omega_0)\right] \\ j\frac{1}{2}\left[h(s+j\omega_0)-h(s-j\omega_0)\right] & \frac{1}{2}\left(g(s+j\omega_0)+g(s-j\omega_0)\right) \end{bmatrix}\begin{bmatrix} i_\alpha(s) \\ i_\beta(s) \end{bmatrix}\end{aligned} \tag{21}$$

Acknowledgment

The authors would like to give their thanks to the graduate student Mr. Gan Weiwei in Xi'an Jiaotong University for his great help in these experiments.

References

[1] B. Singh, K. Al-Haddad, and A. Chandra, "A review of active filters for power quality improvement," Industrial Electronics, IEEE Transactions on, vol. 46, no. 5, pp. 960-971, 1999.

[2] Ortega, J.M.M. Esteve, M.P. Payan, M.B. Exposito, A.G. Franquelo, L.G. , "Reference current computation methods for active power filters: accuracy assessment in the frequency domain," Power Electronics, IEEE Transactions on, vol. 20, no. 2, pp. 446-456, 2005.

[3] C. Donghua and X. Shaojun, "Review of the control strategies applied to active power filters," in Electric Utility Deregulation, Restructuring and Power Technologies, 2004.(DRPT 2004).Proceedings of the 2004 IEEE International Conference on, 2 ed 2004, pp. 666-670.

[4] H. Akagi, et. al, "Instantaneous Reactive Power Compensators Comprising Switching Devices without Engergy Storage Components," IEEE Trans on IA, vol. 20, no.3, pp. 625-630, 1984.

[5] H. Akagi, et al, "Control Strategy of Active Power Filters Using multiple Voltage-Source PWM converters," IEEE Trans. on IA, vol.22, no.3, pp.460-465, 1986.

[6] V. Soares, P. Verdelho, and G. Marques, "A control method for active power filters under unbalanced nonsinusoidal conditions," in Power Electronics and Variable Speed Drives, 1996.Sixth International Conference on (Conf.Publ.No.429) 1996, pp. 120-124.

[7] V. Soares, P. Verdelho, and G.D. Marques, "An instantaneous active and reactive current component method for active filters," Power Electronics, IEEE Transactions on, vol. 15, no. 4, pp. 660-669, 2000.

[8] J.S. Tepper, J.W. Dixon, G. Venegas, and L. Moran, "A simple frequency-independent method for calculating the reactive and harmonic current in a nonlinear load," Industrial Electronics, IEEE Transactions on, vol. 43, no. 6, pp. 647-654, 1996.

[9] F.Z. Peng, H. Akagi, and A. Nabae, "Compensation characteristics of the combined system of shunt passive and series active filters," Industry Applications, IEEE Transactions on, vol. 29, no. 1, pp. 144-152, 1993.

[10] Zmood, D.N. Holmes, D.G. Bode, G.H., "Frequency-domain analysis of three-phase linear current regulators," Industry Applications, IEEE Transactions on, vol. 37, no. 2, pp. 601-610, 2001.

[11] Newman, M.J. Zmood, D.N. Holmes, D.G. , "Stationary frame harmonic reference generation for active filter systems," Industry Applications, IEEE Transactions on, vol. 38, no. 6, pp. 1591-1599, 2002.

[12] R. Pedro, P. Josep, B. Joan, J. I. Candela, P. B. Rolando, and B. Dushan, "Decoupled Double Synchronous Reference Frame PLL for Power Converters Control," Power Electronics, IEEE Transactions on, vol. 22, no. 2, pp. 584-592, 2007.

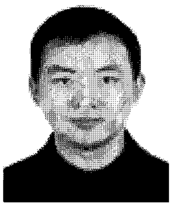

WANG Xiaoyu was born in Shaanxi Province, China in 1979. He received his B.S., M.S. and Ph.D. degrees from Xi'an Jiaotong University, China in 2001, 2004 and 2007 respectively, all in Electrical Engineering. He is currently a Lead Engineer employed by GE (China) Research and Development Center Corporation Limited located in Shanghai, China. His research interests are power quality control, and wind energy.

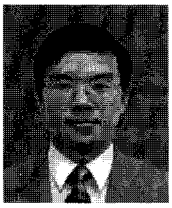

LIU Jinjun was born in Hunan Province, China in 1970. He received his B.S. and Ph.D. degrees from Xi'an Jiaotong University (XJTU), China in 1992 and 1997 respectively. In 1998, he led the founding of XJTU/Rockwell Automation Laboratory. From December 1999 until February 2002, he was with the Center for Power Electronics Systems at Virginia Polytechnic Institute and State University, USA, as a Postdoctoral Research Scholar. He then came back to XJTU and in August of 2002 was promoted to a Full Professor and head of the Power Electronics and Renewable Energy Center at XJTU. Now he is also serving as an Associate Dean of the School of Electrical Engineering at XJTU. He coauthored 3 books, published over 100 technical papers, and received several provincial or ministerial awards for scientific or career achievements and the 2006 Delta Scholar Award. His research interests are power quality control, renewable energy generation and utility applications of power electronics, and modeling and control of power electronic systems. Dr. Liu has served as the IEEE Power Electronics Society Region 10 Liaison for 3 years. He was actively involved in the organization of several power electronic international conferences, including PESC, APEC, IPEC in Japan, ICPE in Korea, and IPEMC in China, as a committee member or co-chair, or as session chair.

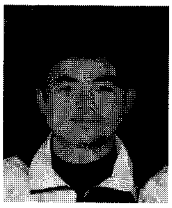

HU Jinku was born in China in 1984. He received his B.S. Degree from Xi'an Jiaotong University, Xi'an, Shaanxi, China in 2006 in Electrical Engineering. He is now a graduate student of Xi'an Jiaotong University in the School of Electrical Engineering. His research interests are modeling and control of power electronics systems and power quality control.

MENG Yuji was born in Hebei Province, China, in 1981. She received her B.S. and M.S. degrees from Xi'an Jiaotong University, Shaanxi, China, in 2003 and 2007, respectively, both in Communication and Information Engineering. She is currently a DSP Architecture Engineer in Marvell Technology Ground Ltd, Shanghai, China. Her research interests are physical layer of communication systems and related digital signal processing.

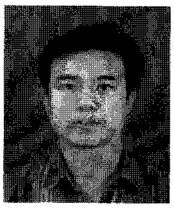

YUAN Chang was born in Hunan, P.R. China, in 1981. He received his B.S. degree in electrical engineering from Xi'an Jiaotong University, Xi'an, Shaanxi, in 2003. He is currently working towards the Ph.D. degree at Xi'an Jiaotong University. His research interests are in the area of power electronics applied in power quality.